Molecular Dynamics Study on Mechanical Responses of Circular Graphene Nanoflake under Nanoindentation

Jeong-Won Kang

Abstract—Graphene, a single-atom sheet, has been considered as the most promising material for making future nanoelectromechanical systems as well as purely electrical switching with graphene transistors. Graphene-based devices have advantages in scaled-up device fabrication due to the recent progress in large area graphene growth and lithographic patterning of graphene nanostructures. Here we investigated its mechanical responses of circular graphene nanoflake under the nanoindentation using classical molecular dynamics simulations. A correlation between the load and the indentation depth was constructed. The nanoindented force in this work was applied to the center point of the circular graphene nanoflake and then, the resonance frequency could be tuned by a nanoindented depth. We found the hardening or the softening of the graphene nanoflake during its nanoindented-deflections, and such properties were recognized by the shift of the resonance frequency. The calculated mechanical parameters in the force-*vs*-deflection plot were in good agreement with previous experimental and theoretical works. This proposed schematics can detect the pressure via the deflection change or/and the resonance frequency shift, and also have great potential for versatile applications in nanoelectromechanical systems.

Keywords—Graphene, pressure sensor, circular graphene nanoflake, molecular dynamics.

I. Introduction

GRAPHENE, a flat monolayer, where carbon atoms are arranged in a hexagonal pattern, is considered as an excellent material for the fabrication of nanoelectromechanical systems (NEMSs) resonators [1]. The associated atomistic interactions are covalently bonded by sp^2 hybridized electrons [2]. Its makeup of strongly bonded planar sheets held together by weak van der Waals interactions makes it relatively simple to fabricate extremely thin resonators, even down to the natural limit of one atomic layer. Graphene possesses exceptional mechanical, electrical, optical and thermal properties, which have made it useful for many applications, such as molecular gas detectors, nanoribbons, transistors, integrated circuits, conductive ultra-capacitors and advanced composites [3]. Beyond its material strength, these materials have gate-tunable conductance, which enables a fully electrical readout of the mechanical motion, chemical inertness and high thermal conductivity in NEMSs [3], [4].

In 2007 Bunch et al. [5] created a prototype for the pressure sensor by placing a graphene flake over a well, after then the pressure sensor based on graphene is a promising development in the class of nanosensors in that it provides unique advantageous electromechanical properties of the graphene [6], many interesting results [7]–[10] have been obtained in this area. Even a small local strain of graphene induced by a single adsorbed molecule was detectable [7]. Several other studies have explored the mechanical [3], [11] and electromechanical response of these systems [12], [13].

In the previous work [6], Kwon et al. presented a novel schematics of the ultrasensitive pressure sensor based on graphene nanoribbons and investigated the electromechanical dynamic operations using classical molecular dynamics (MD) simulations and piezo-electricity theory. In this work, we present an alternative schematic of an ultrasensitive pressure sensor based on graphene using the top plate with a thumbtack-like structure. In order to better understand the potential of this graphene-based pressure sensor, we perform classical MD simulations using the Tersoff-Brenner potential function to investigate its dynamic responses.

II. Simulation Methods

To study the dynamics of the graphene-based pressure sensor, the in-house MD code that was used in our previous work [6] was implemented. This MD code used the velocity Verlet algorithm, a Gunsteren–Berendsen thermostat to control the temperature and neighbor lists to improve the computing performance. The MD time step was 5×10^{-4} ps. We assigned the initial atomic velocities with a Maxwell distribution, and the magnitudes were adjusted in order to fit the temperature of the system. In all of the MD simulations, the temperature was set to 1 K. Interactions between carbons atoms that formed covalent bonds of graphene were modeled using the Tersoff-Brenner potential [14], [15].

Fig. 1 shows a circular graphene nanoflake with a diameter of 6.67 nm composed of 1338 atoms considered in the MD simulations. It was assumed that the border regions of the graphene nanoflake were clamped by an object with a rigid frame as shown in Fig. 1; so the atoms in the boundary region were fixed during the MD simulations whereas the others were treated as the free MD region within the diameter of 6 nm. First, the graphene nanoflake was initially relaxed without external force. Afterwards, the external force was applied to six atoms composed of the center ring of the circular graphene nanoflake. This force increased by 1.6×10^{-4} nN per every 5×10^{-3} ps until breaking.

J. W. Kang is with the Graduate School of Transportation, Korea National University of Transportation, Uiwang 437-763, Republic of Korea, and Department of IT Convergence, Korea National University of Transportation, Chungju 380-702, Republic of Korea (Phone: +82-31-462-8739; Fax: +82-31-462-8734; e-mail: jwkang@ut.ac.kr).
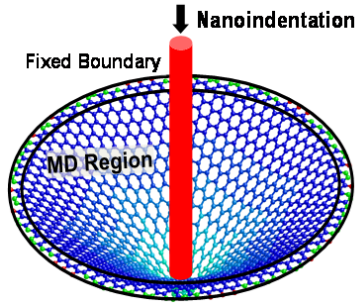
Fig. 1 Schematics for circular graphene nanoflake under the nanoindentation, the circular graphene nanoflake with a diameter of 6.67 nm was composed of 1,338 atoms considered in the MD simulations. It was assumed that the border regions of the graphene nanoflake were clamped by an object with a rigid frame, so the atoms in the boundary region were fixed during the MD simulations whereas the others were treated as the free MD region within the diameter of 6 nm

III. RESULTS AND DISCUSSION

The deflection (w) at the center of the circular graphene nanoflake increased with increasing the applied force. The force-deflection behavior can be approximated as [16]–[18].

$$F_A = \sigma_0^{2D} \pi d \left(\frac{w}{d}\right) + E^{2D} q^3 d \left(\frac{w}{d}\right)^3 \qquad (1)$$

where σ_0^{2D} is the pretension in the film, E^{2D} is the 2-dimentional elastic constant, that is the Young's modulus in 3-dimension, d is the effective diameter, v is Poisson's ratio and 0.12~0.413 in literatures [19], and $q = 1/(1.05 - 0.15v - 0.16v^2)$ is a dimensionless constant [16].

Fig. 2 shows the deflection as a function of the applied force. Inset shows the deflection-vs-force curve in the *log-log* scale. When we compare our MD result and the previous experimental result obtained from an experiment [16], although the sizes of the graphene nanoflake are very different from one another, the trends of both curves are similar.

Considering the difference of the scale between this theoretical work and the previous experimental work [16], the deflection-vs-force curve in this work is in good agreement with that obtained from the experiment [16]. Our MD data were compared to the fitting line using (1). We took $v = 0.413$ and $E^{2D} = 235$ N m^{-1} obtained from the previous works [20], [21] based on the Tersoff–Brenner potential, which is used in this work. It was considered that the pretension σ_0^{2D} is very little and negligible.

We chose the effective diameter $d = 12$ nm to fit the curve, then this value is increased 2 times that of the diameter of the graphene nanoflake in the actual MD simulations. This result can be understood by the extremely hypothetic boundary condition with fixed edge in this MD simulation, which is very different from the real conditions in experiments.
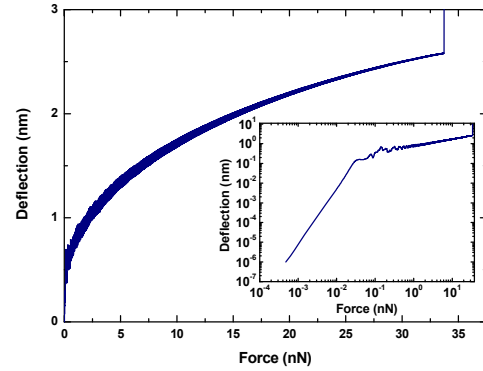

Fig. 2 Deflection *vs.* force plot, inset shows the deflection-*vs*-force curve in the *log-log* scale. The deflection nonlinearly increased with increasing the nanoindentation force

The maximum stress for a clamped, linear elastic, circular membrane under a spherical indenter as a function of the applied load has been derived on the basis of a continuum model as [16]

$$\sigma_M^{2D} = \sqrt{\frac{F_M E^{2D}}{4\pi R}}, \qquad (2)$$

where σ_0^{2D} and F_M are the maximum stress and force at the central point of the film, respectively, and R is the radius of the tip [22]. In this work, the graphene was broken when $F_M = 33.728$ nN and $w_M = 2.609$ nm. Since the applied forces acted on the center hexagon carbon ring in this work, we assumed $2R = 0.496$ nm with the value of the molecular diameter of benzene; then, the intrinsic strength $\sigma_0^{2D} = 50.444$ N m^{-1} could be obtained from (2) using $F_M = 33.728$ nN obtained from this work and $E^{2D} = 235$ N m^{-1} obtained from the Tersoff-Brenner potential [23], [24].

The experimentally determined value of the second-order elastic stiffness for monolayer graphene was $E^{2D} = 340 \pm 50$ N m^{-1} [16]. So when we used $R = 0.496$ nm and $E^{2D} = 340$ N m^{-1}, we obtained $\sigma_0^{2D} = 42.904$ N m^{-1} for the intrinsic strength. These values are in good agreement with the value of $\sigma_0^{2D} = 42 \pm 4$ N m^{-1} obtained from the experiments [16].

The strain (ε) for the bending deflection can be estimated as

$$\varepsilon \approx (w/2R)^2 \qquad (3)$$

by using the approximation for the ribbon [25] or

$$\varepsilon \approx \sqrt{R^2 + w^2}/R - 1 \qquad (4)$$

by using the triangle approximation [6].

The fracture strains approximated by using (3) and (4) are 0.189 and 0.325, respectively. These values are accordant with the experimental fracture strain of 0.25 [16] and the previous theoretical works of 0.165-to-0.382 [26]–[29]. Georgantzinon et al. [26], [27] reported that the fracture strain is 0.257 using the Morse potential and the fracture strain 0.269 using the

molecular mechanics theory. In this work, the ultimate strength is 128 GPa with $\sigma_0^{2D} = 50.444$ N m^{-1} or 150 GPa with $\sigma_0^{2D} = 42.904$ N m^{-1} for the deflective strain, which are compatible with 130 ± 10 GPa of the ultimate strength experimentally [16]. For the uniaxial strains, the ultimate strengths in theoretical studies were 175 GPa by [28] and 120 GPa by [27]. Then, we calculated the effective spring constant (k_{eff}) as a function of the deflection as shown in Fig. 3. The effective spring constant increases with increasing deflection. In this work, the effective spring constant of the circular graphene nanoflake is below ~0.46 N/m. The average effective spring constant is 0.276 N/m. This value is in good agreement with the values of previous works [3], [5], [30]–[33]. Bunch et al. [30] directly measured the effective spring constant to be $k_{eff} = 0.2$ N/m in a graphene membrane by using AFM tip. Frank et al. [3] measured an effective spring constant of 1~5 N/m in suspended multilayered sheets with thicknesses ranging from 2 to 8 nm. Duan and Wang [31] estimated the effective spring constant of a graphene sheet to be approximately 9.85 N/m without the presence of in-plane tension. Bunch et al. [5] measured the effective spring constant to be $k_{eff} = 0.7$ N/m in a 5-nm-thick GNR resonator at room temperature. For GNR resonators, Shivaraman et al. [32] measured the effective spring constant to be $k_{eff} = 0.15~0.4$ N/m by using an AFM tip and the spring constant to be $k_{opt} = 2~4$ N/m of the mode excited by optical resonance measurements. By nanoindentation with an AFM tip, Traversi et al. [33] measured the effective spring constant to be $k_{eff} = 0.07 \sim 0.73$ N/m for samples of suspended mono- and bilayer-GNRs. They presented one sample in detail: its effective spring constant was $k_{eff} = 0.36$ N/m in the linear elastic regime, i.e. the pure bending regime, and as the strain increased into the non-linear elastic regime, the effective spring constant gradually increased to several times higher than that for the linear elastic regime. This trend found by Traversi et al. [33] is in agreement with that in this work, which shows that the effective spring constant gradually increases with increasing deflection.

Sensing the pressures can be achieved from detecting the resonance frequencies as well as the deflections [30]. Bunch et al. [30] demonstrated that the pressure induced strain in the graphene can control the resonance frequency of the suspended graphene. Fig. 4 shows the resonance frequency as a function of the nanoindentation force for ten cases. The resonance frequencies (f_R) increase with increasing applied force. The trend of the resonance frequencies against the applied forces is clearly presented. Bunch et al. [30] discussed that the pressure difference are linearly proportional with the third power of the resonance frequency when the resonance frequencies are sufficiently far from the minimum frequency. Hence, the third power of the resonance frequency is plotted as a function of the applied force as shown in Fig. 4. Then, this relationship can be regressed by the power function $f_R = 1.3843F_A^{0.333}$ as shown in previous experiments [30]. This relationship has been also found in the analysis of the graphene nanoribbon resonators in the computer simulation works [34].
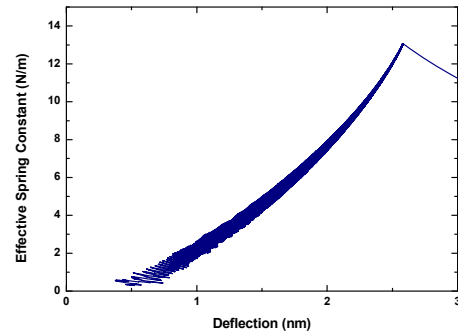

Fig. 3 Effective spring constant *vs* deflection plot, the effective spring constant increases with increasing deflection. In this work, the effective spring constant of the circular graphene nanoflake is below ~0.46 N/m. The average effective spring constant is 0.276 N/m
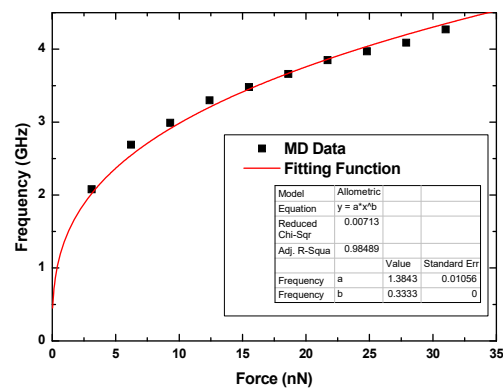

Fig. 4 Resonance frequency *vs.* nanoindentation force plot, the resonance frequencies increase with increasing applied force, then, this relationship can be regressed by the power function $f_R = 1.3843F_A^{0.333}$ as shown in previous experiments [30]. This relationship has been also found in the analysis of the graphene nanoribbon resonators in the computer simulation works [34]

The MD simulation in this work was performed at extremely low temperature, very different from the ordinary conditions for experiments or measurements, so the dynamics features of the circular graphene nanoflake were presented in an ideal situation. However, we can note that the mechanical properties of the circular graphene nanoflake in this work were in good agreement with previous works as discussed above. Hence the results in this work provide meaningful information on the operation of graphene-based pressure sensors. It should be pointed out that a very high level of vacancy is required in such a pressure sensor device to protect the graphene nanoflake sample from the measured environment. Further work should include quantum mechanics to reveal structural and electronic properties of unusual carbon nanostructures, electron transport properties, as well as influence of electric and magnetic fields.

IV. Conclusion

We investigated the mechanical responses of a circular graphene nanoflake, with a view to future engineering application of graphene-based nanoelectromechanical devices

based on classical molecular dynamics simulations and the elastic plate theory. The calculated mechanical parameters in the force-*vs*-deflection plot were in good agreement with previous work. Simulation results for the operations of the studied system were in good agreement with the previous experimental and theoretical works. This proposed schematics can detect the pressure via the deflection change or/and the resonance frequency shift, and also have great potential for versatile applications in nanoelectromechanical systems.

REFERENCES

[1] G. I. Giannopoulos, I. A. Liosatos, and A. K. Moukanidis," Parametric study of elastic mechanical properties of graphene nanoribbons by a new structural mechanics approach," *Physica E*, vol. 44, pp. 124–134, Oct. 2011.

[2] K. S. Novoselov, A. K. Geim, S. V. Morozov, D. Jiang, M. I. Katsnelson, I. V. Grigorieva, S. V. Dubonos, and A. A. Firsov, "Two-dimensional gas of massless Dirac fermions in graphene," *Nature*, vol. 438, pp. 197–200, Nov.2005.

[3] I. W. Frank, D. M. Tanenbaum, A. M. van der Zande, P. L. McEuen, "Mechanical properties of suspended graphene sheets," *Journal of Vacuum Science Technology B*, vol. 25, pp. 2558–2561, Nov./Dec.2007.

[4] V. Sazonova, Y. Yaish, H. Üstünel, D. Roundy, T. A. Arias, and P. L. McEuen, "A tunable carbon nanotube electromechanical oscillator," *Nature*, vol. 431, pp. 284–287, Sep. 2004.

[5] J. S. Bunch, A. M. van der Zande, S. S. Verbridge, I. W. Frank, D. M. Tanenbaum, J. M. Parpia, H. G. Craighead, and P. L. McEuen, "Electromechanical resonators from graphene sheets," *Science*, vol. 315, pp. 490–493, Jan. 2007.

[6] O. K. Kwon, J. H. Lee, K.-S. Kim, and J. W. Kang, "Developing ultrasensitive pressure sensor based on graphene nanoribbon: Molecular dynamics simulation" *Physica E*, vol. 47, pp. 6–11, Jan. 2013.

[7] F. Schedin, A. K. Geim, S. V. Morozov, E. W. Hill, P. Blake, M. I. Katsnelson, and K. S. Novoselov, "Detection of individual gas molecules adsorbed on graphene," *Nature Mater.*, vol. 6, pp. 652–655, July 2007.

[8] C. Y. Wang, K. Mylvaganam, and L. C. Zhang, "Wrinkling of monolayer graphene: A study by molecular dynamics and continuum plate theory," *Phys. Rev. B*, vol. 80, pp. 155445, Oct. 2009.

[9] S. Jun, T. Taxhi, and H. S. Park, "Size-Dependence of the Nonlinear Elastic Softening of Nanoscale Graphene Monolayers Under Plane-Strain Bulge Tests," *J. Nanomater.*, vol. 2001, pp. 380286, 2011.

[10] V. Sorkin and Y. W. Zhang, "Graphene-based pressure nano-sensors," *J. Mol. Mater.*, vol. 17, pp. 2825–2830, 2011.

[11] M. Poot and H. S. J. van der Zant, "Nanomechanical properties of few-layer graphene membranes," *Appl. Phys. Lett.*, vol. 92, pp. 063111, Feb. 2008.

[12] C. Chen, S. Rosenblatt, K. I. Bolotin, W. Kalb, P. Kim, I. Kymissis, H. L. Stormer, T. F. Heinz, and J. Hone, "Performance of Monolayer Graphene Nanomechanical Resonators with Electrical Readout," *Nature Nanotechnol.*, vol. 4, pp. 861–867, Sep. 2009.

[13] K. M. Milaninia, M. A. Baldo, A. Reina, and J. Kong, "All graphene electromechanical switch fabricated by chemical vapor deposition," *Appl. Phys. Lett.*, vol. 95, pp. 183105, Nov. 2009.

[14] J. Tersoff, *Phys. Rev. B*, "Modeling solid-state chemistry: Interatomic potentials for multicomponent systems," vol. 39, pp. 5566–5568, March 1989.

[15] D. W. Brenner, "Empirical potential for hydrocarbons for use in simulating the chemical vapor deposition of diamond films," *Phys. Rev. B*, vol. 42, pp. 9458–9471, Nov. 1990.

[16] C. Lee, X. Wei, J. W. Kysar, and J. Hone, "Measurement of the elastic properties and intrinsic strength of monolayer graphene," *Science*, vol. 321, pp. 385–388, (2008).

[17] K. T. Wan, S. Guo, and D. A. Dillard, "A theoretical and numerical study of a thin clamped circular film under an external load in the presence of a tensile residual stress," *Thin Solid Films*, vol. 425, pp. 150–162, Feb. 2003.

[18] U. Komaragiri and M. R. Begley, "The Mechanical Response of Freestanding Circular Elastic Films Under Point and Pressure Loads," *J. Appl. Mech.*, vol. 72, pp. 203–212, Mar. 2005.

[19] E. Cadelano, P. L. Palla, S. Giordano, and L. Colombo, "Nonlinear elasticity of monolayer graphene," *Phys. Rev. Lett.*, vol. 102, pp. 235502, June 2009.

[20] J. Zhou and R. Huang, "Internal lattice relaxation of single-layer graphene under in-plane deformation," *J. Mech. Phys. Solids*, vol. 56, pp. 1609-1623, Apr. 2008.

[21] M. Arroyo and T. Belytschko, "Finite crystal elasticity of carbon nanotubes based on the exponential Cauchy-Born rule," *Phys. Rev. B*, vol. 69, pp. 115415, Mar. 2004.

[22] N. M. Bhatia and W. Nachbar, "Finite indentation of an elastic membrane by a spherical indenter," *Int. J. Non-Linear Mech.*, vol. 3, pp. 307–324, Sep. 1968.

[23] O. K. Kwon, G.-Y. Lee, H. J. Hwang, and J. W. Kang, "Molecular dynamics modeling and simulations to understand gate-tunable graphene-nanoribbon-resonator," *Physica E*, vol. 45, pp. 194–200, Aug. 2012.

[24] O. K. Kwon, J. H. Lee, J. Park, K.-S. Kim, and J. W. Kang, "Molecular dynamics simulation study on graphene-nanoribbon-resonators tuned by adjusting axial strain," *Curr. Appl. Phys.*, vol. 13, pp. 360–365, Mar. 2013.

[25] A. Isacsson, "Nanomechanical displacement detection using coherent transport in graphene nanoribbon resonators," *Phys. Rev. B*, vol. 84, pp. 125452, Sep. 2011.

[26] S. K. Georgantzinos, G. I. Giannopoulos, D. E. Katsareas, P. A. Kakavas, and N. K. Anifantis, "Size-dependent non-linear mechanical properties of graphene nanoribbons," *Computat. Mater. Sci.*, vol. 50, pp. 2057–2062, May 2011.

[27] S. K. Georgantzinos, D. E. Katsareas, and N. K. Anifantis, "Graphene characterization: A fully non-linear spring-based finite element prediction," *Physica E*, vol. 43, pp. 1833–1839, Aug. 2011.

[28] H. Bu, Y. Chen, M. Zou, H. Yia, K. Bi, and Z. Ni, "Atomistic simulations of mechanical properties of graphene nanoribbons," *Phys. Lett. A*, vol. 373, pp. 3359–3362, Sep. 2009.

[29] H. Zhao, K. Min, and N. R. Aluru, "Size and Chirality Dependent Elastic Properties of Graphene Nanoribbons under Uniaxial Tension" *Nano Lett.*, vol. 9, pp. 3012–3015, Aug. 2009.

[30] J. S. Bunch, S. S. Verbridge, J. S. Alden, A. M. van der Zande, J. M. Parpia, H. G. Craighead, and P. L. McEuen, "Impermeable Atomic Membranes from Graphene Sheets" *Nano Lett.*, vol. 8, pp. 2458–2462, Aug. 2008.

[31] W. H. Duan and C. M. Wang, "Nonlinear bending and stretching of a circular graphene sheet under a central point load," *Nanotechnology*, vol. 20, pp. 075702, Feb. 2009.

[32] S. Shivaraman, R. A. Barton, X. Yu, J. Alden, L. Herman, M. V. S. Chandrashekhar, J. Park, P. L. McEuen, J. M. Par-pia, H. G. Craighead, and M. G. Spencer, "Free-Standing Epitaxial Graphene," *Nano Lett.*, vol. 9, pp. 3100–3105, Sep. 2009.

[33] F. Traversi, F. J. Gúzman-Vázquez, L. G. Rizzi, V. Russo, C. S. Casari, C. Gómez-Navarro, and R. Sordan, "Elastic properties of graphene suspended on a polymer substrate by e-beam exposure," *New J. Phys.*, vol. 12, pp. 023034, Feb. 2010.

[34] J. Atalaya, A. Isacsson, and J. M. Kinaret, "Continuum Elastic Modeling of Graphene Resonators," *Nano Letters*, vol. 8, pp. 4196–4200, Oct. 2008.

Jeong-Won Kang received the B.S., M.S., and PhD. degrees from Chung-Ang University, Seoul, Korea, in 1995, 1997, and 2002, respectively. From 2003 to 2005, he was a visiting professor in Chung-Ang University, from February 2006 to February 2007, he was a research associate in University of California at Riverside, and from October 2007 to February 2008, he worked with a Senior Researcher with LG Siltron. In February 2008, he joined the Department of Computer Engineering, Korea National University of Transportation, Chungju, Republic of Korea, where he is currently an associated Professor. He has authored over 225 peered reviewed papers in various international journals and two book chapters in Encyclopedia of Nanoscience and Nanotechnology published by American Scientific Publishers and Marcel Dekkers Inc. He received a Bronz Medal of Samsumg Human Tech from Samsumg Ltd. (2004), Young Scientist Award from Korean Physical Society (2004), and Outstanding Researcher Award from Korea National University of Transportation (2010, 2014). He served a Committee Member of IEEE NANO 2010, August 2010, Seoul, and Republic of Korea. His main interests are in nano electronic device, semiconductor technology, and process simulation. He has served as one of editorial board member in Journal of Computational and Theoretical Nanoscience, American Scientific Publishers, and Journal of Nanomaterials, Hindawi Publishing Corporation. He has also served as an advisory board member in Journal of High Performance Computing, Bilinfo Publications, Journal of Electrical and Electronic Engineering, Science Publishing Group, and American Journal of Nano Research and Application, Science Publishing Group.